Vietnam Journal of Catalysis and Adsorption
Tạp chí xúc tác và hấp phụ Việt Nam

https://jca.edu.vn

Green synthesis of HAp/CS@β-CD nanocomposite and its applications for bone cell proliferation

Pham Thi Yen Phi, Tran Thi Ngoc Bich, Le Thi Thuy Vi, Phan Trung Kien, Nguyen Van Teo, Pham Xuan Nui*

Department of Chemical Engineering, Hanoi University of Mining and Geology, 18-Pho Vien, Duc Thang, Bac Tu Liem District, Hanoi, Vietnam.
** Email: phamxuannui@humg.edu.vn*

ARTICLE INFO

Received: 10/10/2023
Accepted: 14/11/2023
Published: 30/3/2024

Keywords:
nHAp, nanocomposite, nHAp/CS@β-CD, *Ficus pumila* (L.), cell proliferation

ABSTRACT

In this study, nHAp/CS@β–CD–E nanocomposite has been synthesized by incorporating of chitosan (CS), β-cyclodextrin (β-CD), and *Ficus pumila* (L.) leaf extract with nano-hydroxyapatite (nHAp) via co-precipitation method. Meanwhile, the nHAp obtained from seashells as the starting material sources. The formation of nHAp crystalline phase structure, interfacial interactions, thermal stability and surface structural morphology of nanocomposite samples were characterized by physicochemical methods including XRD, FT-IR, TGA/DTA and SEM, respectively. Investigation of osteoblast cell proliferation activity for the MT3C3-osteoblast cell line was carried out using the MMT method. The results showed that nHAp/CS@β–CD biocomposite has osteoblastic cell proliferation activity, in which the composite contains the *Ficus pumila* (L.) leaf extract has higher activity than composite without extract. This research has new prospects in the field of biomedical material research.

1. Introduction

Biomedical materials are materials of natural or artificial origin, used to replace or perform a vital function of the human body. Typical of which was biomedical porcelain material, a type of material used to replace injured bone parts in the human body without causing harm to the body. Furthermore, this material was also used in cosmetic surgery, dentistry,... [1]. Therefore, the design and development of ideal biomaterial frameworks such as ceramics, polymers, metals and organic bone substitutes must have adequate mechanical properties, biocompatibility, controlled biopermeability, non-toxicity, cost-effectiveness and bioactivity [1]. Some biomedical ceramic materials have been researched and commercialized such as zirconia, bio-glass, zirconia-toughened alumina (ZTA), silicate and the most typically hydroxyapatite (HAp) [2]. Hydroxyapatite, also known as calcium phosphate, was a form of apatite with the chemical formula $Ca_{10}(PO_4)_6(OH)_2$ and was known as a substitute for typical human and animal bones in medicine due to its bioactivity and high biocompatibility with cells. It was one of the versatile materials used for implant purposes due to its similarity to the inorganic mineral composition of the bones of the human body [3–5]. Currently, there have been a number of studies on fabrication of HAp material and its composites for application in bone repair [6,7]. Due to the good bone bonding properties of HAp, it has been widely used in dental and orthopedics surgery to repair bone defects. Combining HAp with chitosan was one of the suitable choices due to its compatibility and high biological

https://doi.org/10.62239/jca.2024.017

activity [8-11]. Chitosan (CS, $(C_6H_{11}O_4N)_n$) was a cationic polyheterosaccharide that was unique in nature consisting of *N*-acetylglucosamine (GlcNAc) and glucosamine (GlcN) moieties, has created orthopedic and biomedical applications. The biological and mechanical properties of chitosan for bone replacement were improved by combining it with HAp [12].

Besides, β-Cyclodextrin (β-CD) was also reported in studies showing that β-CD derivatives have strong bone anabolic effects and aids in bone regeneration. Since β-CD belong to the group of cage molecules whose structural core consists of a size-stable hydrophobic cavity resulting in a "host-guest" relationship that can improve chemical, physical and biological properties of the guest molecule. Therefore, β-CD can be applied in the fields of pharmacy, chemistry, biotechnology, agriculture, medicine,...[13].

Recently, An et al. [14] reported that extract from *Ficus pumila L*. leaves has activity to proliferate bone-forming cells MG-63 in humans. HAp has been synthesized from various starting sources such as eggshells [15], amorphous calcium carbonate [16], calcium lactate pentahydrate and orthophosphoric acid [17], *Venerupis* clam shells [18,19]. Ataka et al. [20] synthesized chitosan, nano-hydroapatite/chitosan composite, and amine group (NH_2) modified nano-hydroxyapatite/chitosan composite for bone tissue engineering. The obtained results show that all synthetic scaffold types have the potential to be used in bone tissue engineering approaches. Mansour et al. [21] studied co-doping Ag^+ and Mg^{2+} into hydroxyapatite/chitosan biocomposite to produce an anti-bacterial effect and improve the mechanical properties of biocomposite. Ghosh et al. [22] used doxorubicin (DOX) to incorporate into hydroxyapatite (HAp)-chitosan (CS) nanocomposite triggered on osteosarcoma cells.

In this study attempt, we have developed a green method for synthesis of biocomposite based on nano-hydroxyapatite (nHAp). Namely, nHAp has been synthesized from seashells and the use of nHAp powder for the fabrication of a biocomposite coating with CS and aqueous extract of *Ficus pumila* (L.) The synthesized biocomposite has been studied by physicochemically through Fourier transform infrared (FTIR), X-ray diffraction (XRD), scanning electron spectroscopy (SEM), and thermogravimetric analysis (TGA) and differential thermal analysis (DTA). The *in-vitro* of the synthesized nanocomposite was assessed through the ability to proliferate MG–63 bone cells.

2. Experimental

Reagents

*Ch*emicals were used in this study including chitosan (CS) with degree of deacetylation (>85%), β-Cyclodextrin (β-CD), C_2H_5OH (99.7%), NaOH (>97%), $(NH_4)_2HPO_4$ (99%), CH_3COOH (99.5%), HCl (37%). Fresh leaves of *Ficus pumila* (L.) were purchased from Lam Dong, Vietnam. Seashell were collected from the wet market in Duc Thang, Vietnam. The chemical reagents were all analytical grade and used without further furification. Deionized water was used in all experiments.

Synthesis of nHAp from seashells

First, seashells were cleaned with tap water, boiled to remove odors, organic matter and impurities. The washed seashells were dried at 100 ^oC for 2 h in an oven. After drying, the seashells were crushed into a fine powder. The crushed sample was heated in furnace at a rate of 5^oC/mim and maintained at 650 ^oC for 3 h to convert calcium carbonate to calcium oxide phase. The sample was then naturally cooled inside the furnance. The calcined powder (CaO) was then used as a calcium source to synthesize nHAp and its biocomposite.

The nHAp fabrication process was carried out as follows: The above 5.27 g of CaO was dissolved in 100 mL of distilled water and stirred continuously to obtain a homogeneous $Ca(OH)_2$ soluttion. To achieve a Ca/P ratio of 0.7, 0.3 M of $(NH_4)_2HPO_4$ was then added to the $Ca(OH)_2$ solution. Then the solution was stirred continously with 450 rpm in a magnetic stirrer for 2 h at room temperature. The mixture was then transferred to autoclave and hydrothermally incubated at 180^oC for 24 h to obtain nano-hydroxyapatite suspension. Next, nano-HAp was filtered and washed several times with distilled water until pH=7 and dried to obtain white powdered nano-hydroxyapatite.

Preparation of Ficus pumila (L.) aqueous extract

The aqueous extract of *Ficus pumila* (L.) was prepared by Soxhlet extraction method. The leaves were washed roughly with tap water for removal of physical dirt. The washed leaves were allowed to dry in sunlight till it dries completely. Then, 100 g of the leaves were grounded into a powder and extracted by the Soxhlet system with a 60:40 (v/v) ratio deionized water and ethanol for 3 h at temperature of 60 ^oC. The extract was left to cool at room temperature before it was filtered using Whatman

https://doi.org/10.62239/jca.2024.017

filter paper. The extract was stored at 4 °C until further use.

Synthesis of nHAp/CS@β-CD-E

1g of CS powder dissolved in 2 wt.% glacial acetic acid solution mixed into 100 mL deionied water and stirred continously for 24 h to obtain a homogeneous suspension (Solution A). Beside, 1 g of nHAp waw dispersed in 100 mL deionied water by sonication for 15 min (Solution B). The β-CD powder (1 g) was also dispersed in 100 mL distilled water by sonication for 15 min (Solution C). The reaction was carried out by mixing the solution A drop-wise into the solution B until the mixture was evenly mixed and then adding the solution C drop-wise into the mixture. The obtained mixture was stirred continuously at 900 rpm for 24 h at room temperature. The product was then filtered and washed several times with deionized water until the filtrate became neutral and dried at 60 °C to obtain nHAp/CS@β-CD.

10 mL of aqueous extract of *Ficus pumila* (L.) was added into 0.1 g of nHAp/CS@β-CD nanocomposite. This mixture was continuously stirred for 2 h at room temperature. The obtained nanocomposite was washed, filtered and dried at 80 ℃ for 24 h, producing the nHAp/CS@β-CD-E powder.

Characterization

X-ray diffraction (XRD) method was measured using a D8 ADVANCE–Bruker (Germany) with Cu-Kα emission with wavelength I=1.5406 Å, power 40KV, current intensity 40 mA, scanning angle 2θ=10−60°. Infrared absorption spectroscopy (FT-IR) was measured on an FT-IR IMPAC-410 (Germany) in the region of 4000-400 cm^{-1}. Scanning electron microscopy (SEM) method was performed by a Hitachi S-4800. Thermal analysis method (TGA-DTA) was measured in the air environment and heated from 30 °C to 800 °C at the rate of 10°C/min.

In–vitro test

Investigation of proliferative activity of MT3C3–E1 cells (mice osteoblasts) by MTT method using tetrazolium salt (MTT–(3–(4,5–dimethylthiazol–2–yl)–2,5–) diphenyltetrazolium)) as a reagent in the colorimetric assay, thereby assessing cell survival and viability. The tetrazolium ring of the reagent adheres tightly to the mitochondria of the active cell. Under the action of dehydrogenase enzyme in the cell, the yellow color of MTT changes to formazan purple.

The test was performed under the condition: insert 190 mL of cells into the wells of a 96-well plate containing 10 µL of reagent. Place the culture plate in the CO_2 incubator at 37°C, 5% CO_2, culture for 72 h. After 72 h, 10 µL of MTT (final concentration of 5 mg/mL) was added to each well. After 4 h, remove the medium, formazan crystals were dissolved with 50 µL (DMSO) 100%. The OD value was measured at 540 nm using a BioTek spectrophotometer. The test was repeated 3 times.

The percentage induction of cell proliferation in the presence of reagents were determined by the following formula:

$$\%\ \text{living cells} = \frac{OD(pattern) - OD(blank)}{OD(DMSO) - OD(blank)} \quad (1)$$

The test was carried out at the Institute of Biotechnology, Vietnam Academy of Science and Technology, 18–Hoang Quoc Viet, Cau Giay, Hanoi, Vietnam.

3. Result and discussion

Characterization of samples

Figure 1 shows the XRD patterns of a as-prepared of nHAp, nHAp/CS, and nHAp/CS@β-CD-E composite. From Figure 1 displays all the diffraction peaks match very well the typical hexagonal structured pure nHAp (JCPDS No. 09–0423). Namely, the diffraction peaks at 2θ=25.9° (002), 31.8° (211), 32.9° (300), 34.1° (202), 39.8° (310), 46.7° (222), 49.5° (213) and 53.1° (004) were the typical feature of nHAp. Besides, all the XRD patterns of the as-synthesized nHAp/CS@β-CD composites match with the polycrystalline structure of nHAp. This result indicated that the nHAp/CS@β-CD biocomposite has been successfully synthesized through grafting reagents into nHAp. However, the peak intensity of nHAp peaks gradually decreased when CS and CS@β–CD–E were coated into nHAp, it was due to chitosan was an organic polymer with poor lattice crystallinity, along with using CS@β-CD-E coated into nHAp can form complexes leading to changes in nHAp structure and properties, where the peaks correspond to the crystal faces.

The average crystalline sizes of the samples were calculated by Scherrer equation: D=kλ/βcosθ (2), where

λ is the wavelength of monochromatic X-ray beam radiation Cu radiation (λ=1.5406 Å), θ is the Bragg's angle, K is a Scherrer constant defined as the crystallite shape and is approximately equal to 0.9. From the Scherrer equation, the crystalline sizes of pure nHAp, nHAp/CS, and nHAp/CS@β-CD-E composite were determined to be 9.4 nm, 13.8 nm and 15.1 nm, respectively.

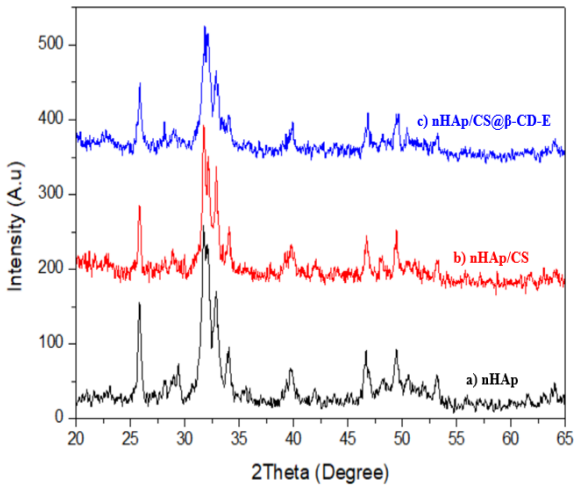

Fig 1: XRD diagram of a) nHAp, b) nHAp/CS and nHAp/CS@β-CD-E samples

The FT- IR spectra (Figure 2) displays the functional groups and chemcial bonds of nHAp, nHAp/CS and nHAp/CS@β-CD.

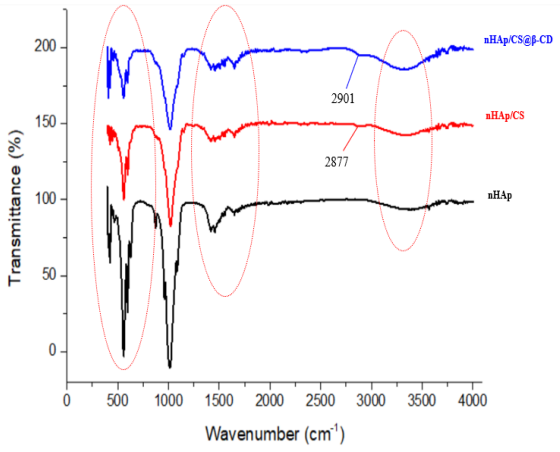

Fig 2: FT-IR spectra of nHAp, nHAp/CS and nHAp/CS@β-CD samples

The broad band observed around 3440 cm^{-1} might ascribed to the O–H stretching vabration on the surface of pure nHAp and nHAp/CS, nHAp/CS@β-CD nanocomposite. The presence of nHAp in CS@β-CD matrix of nHAp/CS@β-CD nanocomposite may reasonably be noticed by appearance of PO_4^{3-} at 1010, 956, 607, 564 and 458 cm^{-1} which are the typical characteristics absorption of nHAp [23]. The bands at 1550–1700 cm^{-1}, which contributed to the N–H primary and secondary amino groups of polymer. Besides, appearance of new bands in range band of 2877 and 2901 cm^{-1} in nHAp/CS, nHAp/CS@β-CD nanocomposite may be assigned to the C–H bond in chitosan. Moreover, the band at 1641 cm^{-1} was attributed to the vibration of C=O [24].

The SEM images of pure nHAp, nHAp/CS and nHAp/CS@β-CD-E nanocomposites (Figure 3) revealed a surface structure morphology. From the SEM images of nHAp (Figure 3(a,b) shows nHAp crystal layers and spherical shape particles. The nHAp/CS SEM image (Figure 3(c,d)) and nHAp/CS@β-CD-E nanocomposites (Figure 3(e,f)) exhibited rougher surface than that of HAp pure and polymer fibers appear on the surface. This may indicate that the nano-rough surface can improve cell adhesion and growth for bone regeneration. Thus, the higher surface nano-roughness of the nanocomposite may facilitate greater cell adhesion and proliferation in it [25].

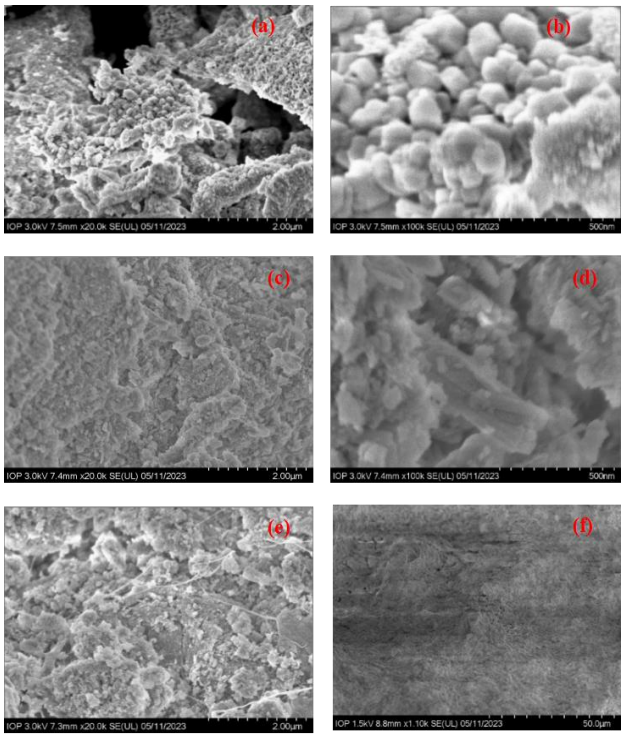

Fig 3: SEM images of (a,b) nHAp, (c,d) nHAp/CS and (e,f) nHAp/CS@β-CD-E samples

In order to study the thermal properties of the composite samples, the thermogravimetric and differential thermal analysis (TGA-DTA) was carried out and the results are shown in Figure 4. From the obtained results show that nHAp pure has a total loss of 11.4% and was divided into two main phases. The first stage lost

https://doi.org/10.62239/jca.2024.017

3.8% of its mass in the temperature range of 25–250 °C due to the loss of surface adsorbed water of the solid material nHAp. The second phase loss of 7.6% mass in the range of 250–800 °C was considered to be the result of the gradual dehydroxylation of nHAp. And in these two stages, no obvious appearance of the peaks was observed to demonstrate the stability of the nHAp material when changing the temperature. Along with that, the mass loss of CS appears in two temperature ranges of 100°C and 272°C corresponding to dehydration and degradation of CS [26]. While the nHAp/CS sample, the total loss was 43.2% and divided into two main phases. The first stage lost 15.3% of its mass in the range of 25–250 °C and the DTA curve appeared the endothermic peak at 60.9 °C. The second stage loses 27.9% of its mass in the range of 250–800 °C and the DTA curve has exothermic peak at 264.8 °C. This shows that nHAp increases the thermal stability of chitosan through the interaction between nHAp and chitosan.

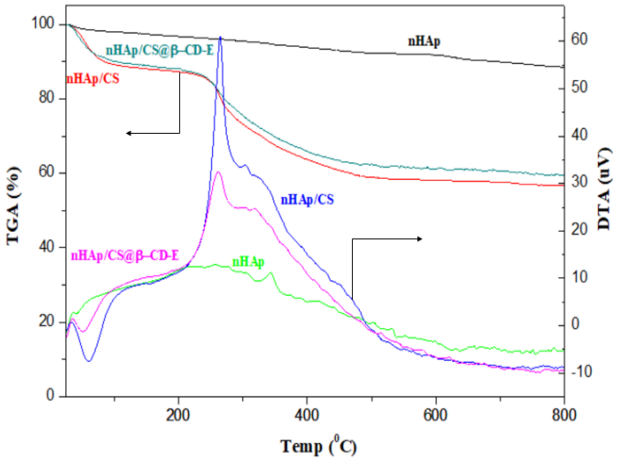

Fig 4: TGA/DTA diagram of nHAp, nHAp/CS and nHAp/CS@*β*-CD-E samples

For the nHAp/CS@β-CD-E nanocomposite had a total loss of 40.3% and divided into two main stages. The first stage loses 12.5% of its mass in the range of 25–250 °C. The second stage loses 27.8% of its mass in the range of 250–800 °C and has exothermic peak at 262.3 °C. It was demonstrated that the combination with β-CD and *Ficus pumila* (L.) leaf extract further improved the thermal stability of the material, specifically, the additional OH groups leading to increased hydrogen bonding between the different components in the material.

Osteoblast proliferation activity assay

To determine the proliferative activity of osteoblasts, the composite samples were tested on the MC3T3-E1 cell line: mouse osteoblasts by the MTT method. The results are shown in Table 1 and the ability to induce cell proliferation of the material is shown in Figure 5.

From the obtained results show that nHAp/CS@β–CD–E sample has the same concentration as nHAp/CS@β–CD and nHAp/CS composites but has a higher percentage of living cells than the other two samples, although the percentage of living cells was not extremely high at the investigated concentrations. However, nHAp/CS@β–CD–E nanocomposite may have a higher percentage of viable cells when investigated at lower concentrations. Thus, it can be seen that biocomposite based on nHAp/CS@β–CD–E sample has higer ability to proliferate osteoblastic cells than the nHAp/CS sample without the extract. And this will be investigated in further studies.

Table 1: Ability to induce cell proliferation of composite samples

Concentration	nHAp/CS@β-CD –E		nHAp/CS@β -CD		nHAp /CS	
	% alive	Error	% alive	Error	% alive	Error
1 mg/mL	91.25	5.25	88.95	6.55	85.39	1.68
0.5 mg/mL	103.74	4.17	96.74	5.03	92.38	3.89
0.1 mg/mL	104.23	5.11	98.98	3.14	96.97	4.67
0.05 mg/mL	105.67	3.31	104.41	2.67	102.20	1.91
Negative control	100.00	6.31				

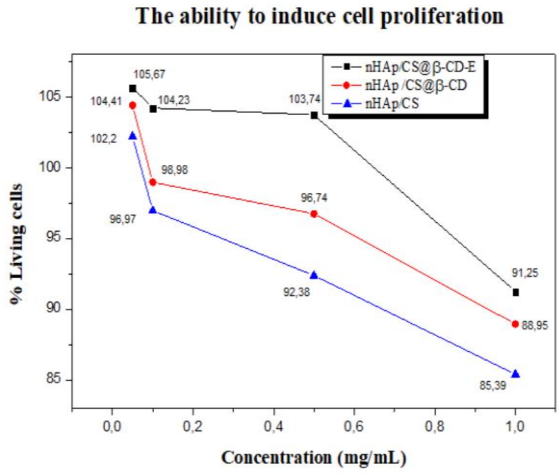

Fig 1: Ability to induce cell proliferation of composite samples

4. Conclusions

The XRD patterns showed the formation of nHAp spherical crystalline particles. The increase in size of nHAp/CS@β-CD-E upon incorporation of CS and β-CD-E compared to nHAp pure. The FT–IR spectra displayed a intermolecular interaction between the

https://doi.org/10.62239/jca.2024.017

components of CS, β-CD with nHAp in nHAp/CS@β-CD-E nanocomposite. Roughness in morphological surface of nHAp/CS@β-CD-E nanocomposite was observed through SEM images leading to improve cell adhesion and growth for bone regeneration. Investigation of osteoblast proliferation activity of biocomposite showed bone-forming cell proliferation activity on cell line MT3C3. In conclusion, we had sucessfully developed β–CD–E loaded nHAp/CS, which may have potential application in a bone repairing systems.

Acknowledgments

This research was supported by the Young Talent Fund of the University of Mining and Geology.

References

1. B.X. Vuong, U.N. Huy, M.T. Tuyet, V.O. Kieu, B.T. Hoa, Hue University Journal of Science (HU JOS) 92(4), 2014.
2. F. Baino, G. Novajra, V. Miguez-Pacheco, A.R. Boccaccini, C. Vitale-Brovarone, J. Non. Cryst. Solids 432 2016) 15–30. https://doi.org/10.1016/j.jnoncrysol.2015.02.015
3. B.X. Vương, VNU Journal of Science 34 (2018) 9-15. https://doi.org/10.25073/2588-1140/vnunst.4689
4. S.-L. Bee, Z.A.A. Hamid, Ceram Int. 46 (2020) 17149–17175. https://doi.org/10.1016/j.ceramint.2020.04.103
5. H.Q. Phong và cộng sự, Tạp chí Khoa học Trường Đại học Cần Thơ 56 (2020) 199–211. https://doi.org/10.22144/ctu.jsi.2020.056
6. T. Kokubo, H.M. Kim, M. Kawashita, Biomaterials 24 (2003) 2161–2175. https://doi.org/10.1016/S0142-9612(03)00044-9
7. A.M. Martins, C.M. Alves, F.K. Kasper, A.G. Mikos, R.L. Reis, J. Mater. Chem. 20 (2010) 1638–1645. https://doi.org/10.1039/B916259N
8. V.C. Dumont, H.S. Mansur, A.A.P. Mansur, S.M. Carvalho, N.S.V. Capanema, B.R. Barrioni, Int. J. Biol. Macromol. 93 (2016) 1465-1478. https://doi.org/10.1016/j.ijbiomac.2016.04.030
9. D. Gopi, S. Nithiya, E. Shinyjoy, D. Rajeswari, L. Kavitha, Ind. Eng. Chem. Res. 53 (2014) 7660–7669. https://doi.org/10.1021/ie403903q.
10. B. Lowe, J. Venkatesan, M.S. Shim, S.K. Kim, Int. J. Biol. Macromol. 93 (2016) 1479-1487. https://doi.org/10.1016/j.ijbiomac.2016.02.054
11. K. Pandi, N. Viswanathan, Carbohydr. Polym. 134 (2015) 732–739. https://doi.org/10.1016/j.carbpol.2015.08.003
12. M. Shakir, R. Jolly, M.S. Khan, A. Rauf, S. Kazmi, Int. J. Biol. Macromol. 93 (2016) 276–289. https://doi.org/10.1016/j.ijbiomac.2016.08.046
13. X.-M. Liu, A.T. Wiswall, J.E. Rutledge, M.P. Akhter, D.M. Cullen, R.A. Reinhardt, D. Wang, Biomaterials 29(11) (2008) 1686–1692. https://doi.org/10.1016/j.biomaterials.2007.12.023
14. N.H. An et al., *Sở Khoa học và Công nghệ TP.Hồ Chí Minh, chương trình Vườn ươm Sáng tạo Khoa học và Công nghệ*, 2017.
15. P.X. Nui, P.T. Ngan, N.T. Hoa, T.T. Thanh-Huong, N.T. Phuong-Lan, T.T. Van-Thi, Vietnam Journal of Catalysis and Adsorption 8(2) (2019) 74-80.
16. M. Sawada, K. Sridhar, Y. Kanda, S. Yamanaka, Scientific Reports 11 (2021) 11546. http://doi.org/10.1038/s41598-021-91064-y
17. P. Szterner, M. Biernat, Bioinorg. Chem. Appl. 2 (2022) 1-13. https://doi.org/10.1155/2022/3481677
18. S. Bramhe, T.N. Kim, A. Balakrishnan, M.C. Chu, Mater. Lett. 135 (2014) 195–198. https://doi.org/10.1016/j.matlet.2014.07.137
19. X. Zhang, K.S. Vecchio, Mater. Sci. Eng. C 26(8) (2006) 1445–1450. https://doi.org/10.1016/j.msec.2005.08.007
20. B.H. Ataka, B. Buyuk, M. Huysal, S. Isika, M. Senel, W. Metzger, G. Cetin, Carbohydr. Polym. 164 (2017) 200–213. https://doi.org/10.1016/j.carbpol.2017.01.100
21. S.F. Mansour, S.I. El-dek, S.V. Dorozhkin, M.K. Ahmed, New J. Chem. 41(22) (2017) 13773-13783. https://doi.org/10.1039/C7NJ01777D
22. S. Ghosh, S. Ghosh, N. Pramanik, Adv. Compos. Hybrid Mater. 3 (2020) 303 - 314. https://doi.org/10.1007/s42114-020-00154-4
23. T. Xu, R. Zou, X. Lei, X. Qi, Q. Wu, W. Yao, Q. Xu, Appl. Catal. B: Environ. 245 (2019) 662–671. https://doi.org/10.1016/j.apcatb.2019.01.020
24. F.M. Queiroz, T.R.K. Melo, A.D. Sabry, L.G. Sassaki, O.A.H. Rocha, Mar. Drugs 13 (2014) 141–158. https://doi.org/10.3390/md13010141
25. I. Zia, R. Jolly, S. Mirza, A. Rehman, M. Shakir, Chemistry Select 7 (2022) 1-10. https://doi.org/10.1002/slct.202103234